Journal of Network Intelligence
Taiwan Ubiquitous Information
 ISSN 2414-8105
Volume **10**, Number **3**, August **2025**

Research on Image Registration Method Based on Feature Operator and Improved Meta-Heuristic Algorithm

Hui-Yan Zhao[1,*], Jin-Chao Zhao[2], Zhou-Xiang Zhen[3]

[1]Zhengzhou Shengda University, Zhengzhou 451191, P. R. China
xczhyan@163.com

[2]Zhengzhou University of Light Industry, Zhengzhou 450000, P. R. China
zhaojinchao101@163.com

[3]Faculty of Information Science and Technology, National University of Malaysia, Selangor 43600, Malaysia
100618@shengda.edu.cn

[*]Corresponding author: Hui-Yan Zhao

Received May 8, 2024, revised October 24, 2024, accepted January 11, 2025.

Abstract. *Image registration is a technique to find the correspondence of common regions of two or more images that contain common regions. Image registration has important applications in medical imaging, remote sensing imaging, machine vision and other fields. A good image registration method needs to be accurate, robust and computationally efficient. Therefore, an image registration method based on feature operator and improved meta-heuristic algorithm is proposed. Firstly, the basic principles of differential evolutionary algorithm and SURF algorithm are analysed. Then, the SURF algorithm is used for feature point detection, and the feature principal direction is determined by Haar wavelet template, and the feature operator is constructed after the feature principal direction is obtained. Since the traditional SURF algorithm uses rectangular operators up to 64 dimensions, it leads to a very large amount of computation and is not robust. Therefore, it is proposed to use DAISY circular operator to replace the rectangular operator in the original algorithm, which reduces the 64-dimensional operator to 25-dimensional operator, and this structure makes the robustness greatly enhanced and reduces the computational complexity. Secondly, a differential evolution method based on Hausdorff distance is proposed to achieve feature point matching. In addition, in order to further optimise the performance of the differential evolution algorithm in image registration, an adaptive strategy, a simulated annealing algorithm and a normally distributed random function are introduced to adaptively update the key parameters. Finally, simulation tests are performed on image samples with different image qualities (focus blur, zoom, rotation and viewpoint change, etc.). The experimental results show that the proposed algorithm has an average accuracy of 0.9662 and an average RMSE of 0.5082, obtaining high accuracy and robustness.*
Keywords: Image registration; SURF algorithm; DAISY feature operator; Differential evolutionary algorithm; Hausdorff distance

1. **Introduction.** Image registration is a technique used to find the correspondence between common regions of two or more images that contain common regions [1]. The images to be aligned can come from the same or different sensors and imaging devices, shooting angles, and shooting times. Image registration technology is a key research direction in the field of image processing and computer vision research. Image registration

is mainly applied to remote sensing image processing, medical image processing, image and video pattern recognition, target retrieval and other fields [2, 3, 4, 5]. The results of image registration directly affect the subsequent tasks such as image stitching, pattern recognition, and target detection. Therefore, the research and exploration of image registration algorithms have important theoretical research and social application value.

Image registration techniques originated in the 1870s in areas such as aircraft navigation and missile terminal guidance [6]. In the registration process, the feature-based registration approach has been studied more because it is less dependent on the surrounding environment of the image and the shooting light, and its features are stable in the image itself, which is often used as the focus of the registration analysis [7, 8]. However, as image features are easily affected by noise, it also brings challenges to the feature-based registration approach. In the feature registration process, there are three main perspectives: feature points, feature regions and feature edges [**?**], of which feature point-based registration is generally more accurate, although it is costly. The image registration process mainly includes image preprocessing, image feature point retrieval, image feature point description, image feature point pair matching, and image transformation. Image fusion through image registration technology can effectively solve the problem of large field of view fisheye lens shooting images with serious negative distortion, but also can effectively solve the traditional way to take the camera ring shot to get the panoramic image distortion distortion is large distortion obvious problem.

1.1. **Related work.** Region model-based image registration algorithms and feature model-based image registration algorithms are two mainstream methods in the related research field at present. The former obtains the transformation relationship between images through the correspondence between the contents, features and structures of the same region between different images, and then can be used for image registration and other processes [9]. The latter is through the qualitative and quantitative analysis of the local features of the image, rather than using a region-based global image registration method, so the amount of computation is greatly reduced and the efficiency is improved accordingly [10]. The hybrid model-based image registration algorithm can simultaneously adopt the registration methods of the above two approaches, thus taking into account the registration accuracy and operational efficiency. In addition, the hybrid model-based image registration algorithm has good stability to the relative displacement or rotation changes, brightness or scale changes, and visual transformations of the image. In this paper, the research on image registration techniques focuses on the improvement of the hybrid model.

Wu et al. [11] proposed a fast and fully automatic registration method for multi-source remote sensing images using point features. Firstly, the SIFT operator with scale invariance and affine transform model are used to roughly match the multi-source remote sensing images. After unifying the size of the image scale space, the Harris corners are obtained from the wavelet domain for fine matching, which achieves the fast and automatic registration of multi-source remote sensing images. Hong and Zhang [12] proposed a wavelet-based registration algorithm for high-resolution remote sensing images. Firstly, the matching point pairs are obtained by normalised correlation algorithm, and then the probabilistic relaxation method is used to kick out the mismatched point pairs, so that the discrete wavelet transform and the redundant wavelet transform are integrated into a single registration process. Liu et al. [13] proposed a registration algorithm for SAR images with affine invariant SIFT features. Firstly, the feature operators in classical SIFT are replaced by SIFT feature operators with affine invariant features. Then the coarse matching is performed to get the coarse matching transform matrix, and the Singular

Value Decomposition (SVD) is used for the fine matching to get the fine matching transform matrix, which achieves a higher registration accuracy. Singleton et al. [14] proposed an InSAR image registration method based on the fast offset estimation. The SURF algorithm and Fast-LTS are used in the first matching stage, and then the conventional normalised correlation algorithm is used to fine-match the images, which can achieve the pixel-level registration effect. Wu et al. [15] proposed a registration method combining the Harris algorithm and the SURF algorithm. In the initial matching stage, the threshold evaluation method and the SURF operator are used, and the stochastic consistency algorithm is used to eliminate the mismatched pairs. The coarse matching results are used to construct a triangular network, and then the fine matching is performed using the similar triangle restriction and Harris corner detection algorithm. Good matching efficiency is obtained on UAV images, but the method is complex and has the problems of weak robustness and low efficiency.

1.2. **Motivation and contribution.** The traditional SURF algorithm uses up to 64-dimensional feature descriptors in the feature description stage, which leads to high complexity, high computational effort, and low correctness of the final matching results. Therefore, this work tries to improve the feature operator of SURF algorithm. As a result, this work proposes an image registration method based on feature operators and improved meta-heuristic algorithms. The main innovations and contributions of this work include:

(1) Aiming at the problems of the traditional SURF algorithm, which is not robust and has a low accuracy rate, an improved feature operator is proposed. The SURF algorithm, after obtaining the feature principal direction in the feature description stage, uses the 25-dimensional DAISY operator [16, 17] to replace the 64-dimensional SURF operator, thus reducing the computational complexity. In addition, the M-Estimate Sample Consensus (MSAC) algorithm [18] is chosen to replace the Random Sample Consensus (RANSAC) algorithm [19] in the process of elimination of mismatched point pairs to enhance robustness.

(2) Aiming at the problems of poor robustness and low global optimisation ability of nearest neighbour KNN matching method based on Euclidean distance, a feature point matching method based on Hausdorff distance [20] and differential evolution (DE) algorithm [21, 22] is proposed. In order to further optimise the performance of the DE algorithm in image registration, an adaptive strategy is introduced for the differential scaling factor and the crossover probability is randomly updated using a normal distribution.

2. Analysis of relevant principles.

2.1. **Basic principles and characteristics of DE algorithm.** DE algorithm is a kind of group intelligence-based, stochastic heuristic global search algorithm, which belongs to a kind of evolutionary algorithm. In DE algorithm, by simulating the process of biological evolution, the solution of the problem is optimised gradually by means of continuous evolution. Compared with other evolutionary algorithms, DE algorithm has lower computational complexity and better global search ability. Its core idea is to iteratively optimise by randomly generating and manipulating the difference vectors of individuals, and using the difference vectors to update the individuals. The DE algorithm has a wide range of applications in solving complex optimisation problems, such as in the fields of function optimisation, combinatorial optimisation, parameter optimisation, etc. It can be used to solve complex optimisation problems by means of global search. It searches for the optimal solution by means of global search, which leads to high solution efficiency and accuracy in practical problems.

The DE algorithm steps consist of four main parts [23]: initialisation of the population, mutation operation, crossover operation and selection operation.

Step 1: Initialise the population

First, the population size NP and the population dimension D (number of decision variables) are determined. After that, a uniformly distributed random function is used to generate the initial population.

$$X_i(0) = (x_{i,1}, x_{i,2}, \ldots, x_{i,D}) \tag{1}$$

$$x_{i,j} = a_j + \text{rand}(b_j - a_j) \tag{2}$$

where $i = 1, 2, \ldots, NP$; $j = 1, 2, \ldots, D$; $X_i(0)$ denotes the i-th individual of the initial population; $x_{i,j}$ denotes the j-th component of the i-th individual; $a_j \leq x_{i,j} \leq b_j$.

Step 2: Mutation operation

The mutation operation is a key step in generating individuals for the intermediate generation of the population. Three different individuals x_{r1}^G, x_{r2}^G, x_{r3}^G are randomly selected from the current population, and G denotes the number of generations of the current population. Generate the difference vector $D_{r1,2}^G$ based on the difference of two individuals:

$$D_{r1,2}^G = x_{r1}^G - x_{r2}^G \tag{3}$$

A new individual is generated as:

$$v_i^{G+1} = x_{r3}^G + F(x_{r1}^G - x_{r2}^G) \tag{4}$$

where F is a real constant on $[0, 2]$ controlling amplification of the difference vector.

Step 3: Crossover operation

The new individual v_i^{G+1} generated during the mutation operation is crossed with the i-th individual of the population x_i^G to generate an experimental individual:

$${U_{i,j}}^{G+1} = \left({u_{i,1}}^G, {u_{i,2}}^G, \ldots {\mu_{i,j}}^G\right) \quad j = 1, 2, ..D \tag{5}$$

$$u_{i,j}^{G+1} = \begin{cases} v_{i,j}^{G+1}, & \text{if rand} \leq CR \text{ or } j = j_{\text{rand}} \\ x_{i,j}^G, & \text{otherwise} \end{cases} \tag{6}$$

where $CR \in (0, 1)$ is the crossover probability factor, j_{rand} is a random integer in $[1, D]$.

Step 4: Selection Operation

The experimental individuals compete with the target individuals generated after mutation and crossover operations to determine the individuals that will become the next generation of the population:

$$x_i^{G+1} = \begin{cases} u_i^{G+1}, & \text{if } f(u_i^{G+1}) \leq f(x_i^G) \\ x_i^G, & \text{else} \end{cases} \tag{7}$$

where f is the fitness function.

Repeat the above steps until the termination condition is met.

The main features of the DE algorithm compared to other traditional optimisation algorithms are [24]:

(1) The DE algorithm is encoded in real numbers and is suitable for optimisation problems on continuous spaces.

(2) The DE algorithm uses probabilistic transfer rules and does not require deterministic rules. Under the same accuracy requirement, the DE algorithm has a faster convergence speed than other optimisation algorithms.

(3) The DE algorithm has few parameters, and a simple parameter control strategy can achieve satisfactory optimisation results, and it is good at solving high-dimensional

function optimisation problems, which is suitable for processing high-dimensional feature operators (64-dimensional feature operators in SURF) in the image registration task.

(4) The DE algorithm operates directly on structural objects without qualification of the objective function, and has an extremely strong group search capability and the ability to memorise individual optimal solutions.

2.2. **Principle of SURF algorithm.** The SURF algorithm is a fast and robust feature extraction algorithm based on the STFT algorithm [25]. This method, in order to improve the speed of detecting feature points, streamlines and enhances the Gaussian second-order differential template, which converts the image filtering process into a simple addition and subtraction operation. This approximate simplified operation is independent of the size of the filter template and improves the feature point detection speed by about three times compared to the SIFT algorithm.

The SURF algorithm converts complex image filtering operations into simple mathematical addition and subtraction operations using integral image and box filtering. The integral is defined as the value $ii(x, y)$ at any point (x, y) in the image. The value $ii(x, y)$ is the sum of the grey values of all points in the rectangular region formed by the upper left corner of the source image to the point (x, y):

$$ii(x, y) = \sum_{x' \le x, y' \le y} p(x', y') \tag{8}$$

where $p(x', y')$ denotes the grey value of the point (x', y') in the original image, and $ii(x, y)$ denotes the integral image.

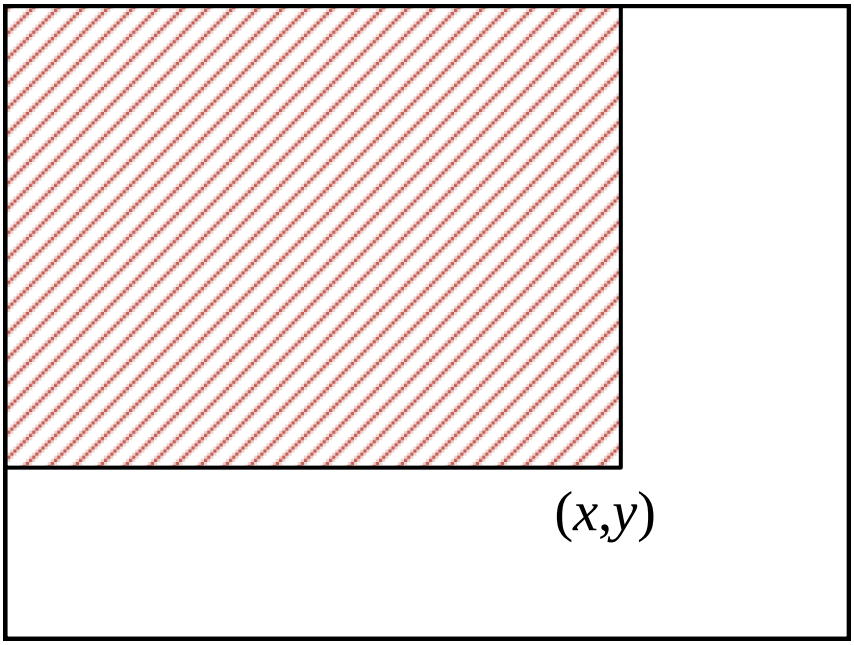

Figure 1. Integral image

SURF algorithm feature point detection and SIFT algorithm feature point detection method is basically the same, are through the use of Hessian matrix to find the feature points of the image. For a point (x, y) in an image I, the Hessian matrix $H(x, \sigma)$ with scale σ is calculated as follows.

$$H(x, \sigma) = \begin{bmatrix} L_{xx}(x, \sigma) & L_{xy}(x, \sigma) \\ L_{xy}(x, \sigma) & L_{yy}(x, \sigma) \end{bmatrix} \tag{9}$$

$$g(\sigma) = \frac{1}{2\pi\sigma} e^{\frac{(x+y)^2}{2\pi\sigma}} \tag{10}$$

where $L_{xx}(x, \sigma)$ denotes the convolution of the Gaussian second-order differential $\frac{\partial^2 g(\sigma)}{\partial x^2}$ with the image I at the point (x, y).

For feature description, the principal direction of each SURF feature point is represented by a Haar wavelet convolution weighted by a Gaussian distribution in the x and y directions. The Gaussian weighting is based on the distance from the pixel point to the feature point, with closer distances having a higher weight and farther distances from the feature point having a lower weight. A sliding $\pi/3$ sector of radius 6σ (σ is the size of the filter) centred on the current feature point is used to scan the wavelet response of the circular region here. The sector with the largest sum of wavelet responses is identified as the feature principal direction.

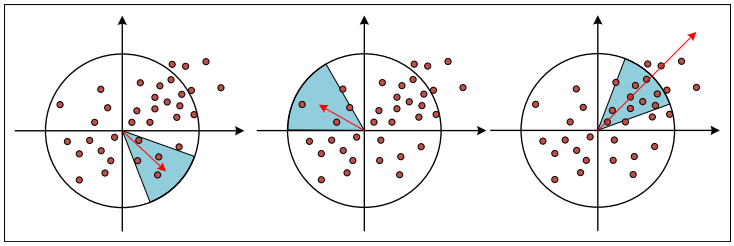

Figure 2. Schematic representation of the main orientation of the feature points.

Establish a coordinate system based on the feature points and their principal directions, and construct a rectangle with a side length of 20σ. The rectangle is partitioned into 16 sub-regions with side lengths of 5σ. For each sub-square region, a Harr template of size 2σ is used to calculate the response value. The Haar wavelet responses dx and dy are computed for each pixel point in the x and y directions, and weights are assigned to them to improve the robustness of the algorithm. Then, the response values and absolute values of each region are summed separately to obtain $\sum dx$, $\sum |dx|$, $\sum dy$, and $\sum |dy|$.

3. Image registration based on SURF and variable parameter DE.

3.1. Improved feature operators.

The SURF algorithm uses the DAISY operator to replace the 64-dimensional feature operator in SURF after obtaining the feature principal directions in the feature description stage. Unlike SIFT and SURF which use rectangular neighbourhood, DAISY algorithm uses circular neighbourhood because circular neighbourhood has better localization properties.

The DAISY operator uses Gaussian kernel convolution to complete the gradient histogram weighting, due to the isotropy of the Gaussian kernel, there is no need to repeat the calculation of the gradient histogram. Take a sampling point every 45 degrees, and get a total of 25 sampling points. The DAISY operator can easily obtain the rotational invariance, so the DAISY operator is chosen to replace the one in the SURF algorithm. An expression for the DAISY operator can be obtained as follow:

$$\frac{\partial^2 H}{\partial x^2}, \quad \frac{\partial H}{\partial x} \tag{11}$$

The vector S needs to be normalised.

$$S = \frac{S}{\|S\|} \tag{12}$$

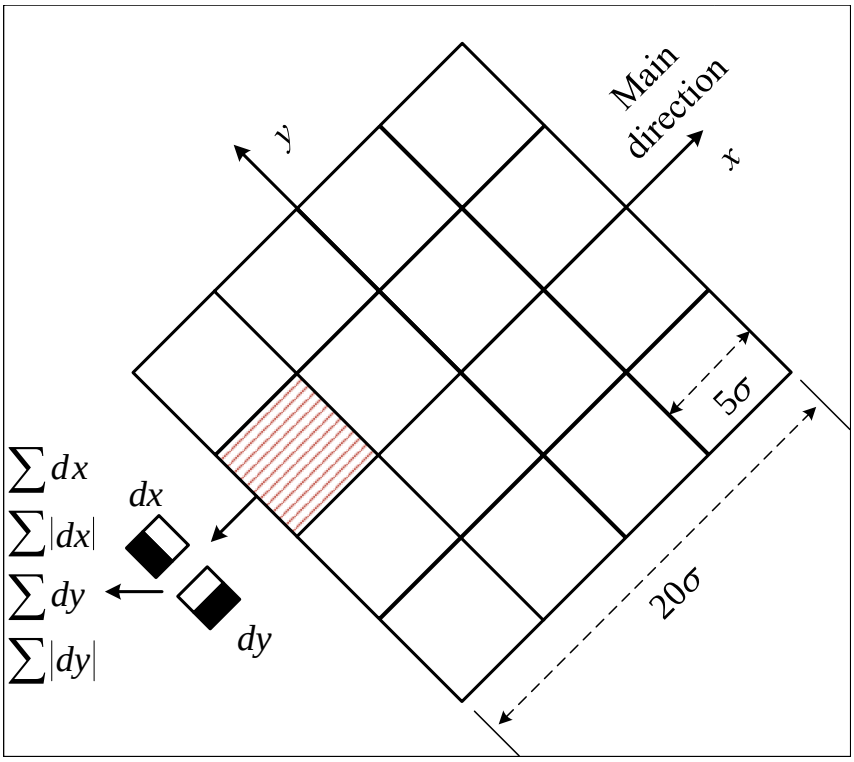

Figure 3. Construction of feature descriptions

Even if there is an error in the assignment of the main direction of the feature points, the computation area is still a concentric ring area, and no additional computation is needed, thus realizing the purpose of reducing the amount of computation and reducing the feature description time.

3.2. **Mismatch Removal.** No matter what kind of feature matching algorithm is used, the matched feature pairs will always contain a certain amount of mis-matched pairs, and the existence of mis-matched pairs will directly affect the quality of image fusion after registration, so it is necessary to remove the mis-matched pairs. The traditional algorithm for the elimination of mismatched pairs uses the Random Sample Consensus (RANSAC) algorithm, while this paper chooses to use the M-Estimate Sample Consensus (MSAC) algorithm. The RANSAC algorithm is basically the same as the MSAC algorithm, but the main difference lies in the different ways of calculating the Consensus Cost. From the point of view of the overall operation effect and the stability of the programme, the MASC algorithm is better than the RANSAC algorithm.

The final result of the RANSAC algorithm depends on the number of randomly selected interior points m and the number of iterations n. If the value of m is too large, the model obtained from each loop will be consistent, i.e., the existence of the value of m is meaningless, and if the value of m is too small, the model parameters obtained will be unstable. The MSAC algorithm is an improved algorithm to address this problem. The selection of the iteration number n mainly affects the running time and the final results.

3.3. **Variable parameter DE algorithm.** As a meta-heuristic algorithm based on swarm intelligence, the Differential Evolutionary Algorithm (DE) can achieve a global optimal solution with strong stability under the condition that only a small number of adjustment parameters are required. The main parameters F and CR of the conventional DE algorithm are set to fixed values during the initialisation of the algorithm, which may lead to the DE algorithm being prone to premature convergence, resulting in a decrease

in accuracy, and at the same time requiring a large amount of search time. Therefore, this paper proposes a Variable Parametric Differential Evolution (VPDE) algorithm with the following improvements:

Since the performance of the traditional DE algorithm is very sensitive to the size of the adjustment factor, it is easy to fall into the local optimum. Therefore, in this paper, the DE algorithm is improved by using the simulated annealing algorithm, which modifies the way of population updating so as to improve the algorithm's global searching ability, as shown below:

$$p(i,j) = q \cdot x(r(i,1),j) + (1-q) \cdot x(rb,j) \tag{13}$$

$$q = \frac{t_{\max} - t}{t_{\max}} \tag{14}$$

where $q \in [0,1]$ denotes the annealing factor, t denotes the current number of iterations, $t_{\max}$ is the maximum number of iterations, and $x(rb,j)$ denotes the global optimum.

By dynamically adjusting the crossover probability, the DE algorithm can better balance the ratio of exploration and exploitation during the search process and improve the search efficiency. Therefore, in this paper, the crossover probability CR is randomly updated using a normal distribution in order to successfully generate new CR with excellent information for the next generation, which is generated as follows:

$$CR_i = \text{randn}(\mu_{CR}, 0.1) \tag{15}$$

$$\mu_{CR} = (1-c) \cdot \mu_{CR} + c \cdot \text{mean}_A(S_{CR}) \tag{16}$$

where S_{CR} is the set of CR that have successfully produced the next generation of individuals, and $\text{mean}_A(\cdot)$ denotes a function that seeks the arithmetic mean. The normally distributed stochastic update can adaptively adjust the size and range of variation of the crossover probability according to the current progress of the search.

Compared with CR parameter, F value has more influence on DE algorithm, to find the optimal value of F in practice, so adaptive variable parameter method is adopted. Assuming that $F_{\min} = 0$ and $F_{\max} = 2$, the F value at each generation of evolution satisfies:

$$F = F_{\min} + (F_{\max} - F_{\min}) \cdot e^{(1-G/G_{\max})} \tag{17}$$

where G is the current generation, $G_{\max}$ is the maximum.

3.4. **Feature point matching based on Hausdorff distance and VPDE.** Similar to SIFT algorithm, SURF algorithm uses nearest neighbour KNN matching based on Euclidean distance. Firstly, we need to find the feature points with similarity between the two images, and then establish the mapping relationship between the points, then the two images can be matched. The nearest neighbour matching method based on Euclidean distance firstly needs to calculate the distance between the feature vectors of the feature points in the reference image and the feature vectors of the feature points on the target image, i.e. Euclidean distance.

$$d = \sqrt{\sum_i (x_{i1} - x_{i2})^2} \tag{18}$$

where i denotes the dimension, and x_{i1} denotes the ith dimension coordinate of the first image.

Assuming that R_i denotes the feature point vector of the image to be matched, and S_j denotes the feature point vector of the reference image, the distance calculation method is shown below:

$$d(R_i, S_j) = \sqrt{\sum_k (R_{i,k} - S_{j,k})^2} \tag{19}$$

The SURF operator for feature matching using Euclidean distance introduces a comparison of Hessian matrix traces. If the sign of the matrix trace of two matched points is the same, it means that these two feature points have contrast variation in the same direction, and vice versa, it means that these two feature vectors are different in direction, and the Euclidean distance is zero, which can be directly eliminated.

However, nearest-neighbour KNN matching methods based on Euclidean distance suffer from poor robustness and low global optimisation capability. For example, when there is noise in the image or the keypoints are not extracted accurately, the Euclidean distance may lead to incorrect matching, which affects the final registration result. Poor robustness may lead to unstable registration results. A common improvement approach to the above problem is to introduce more complex feature representations, such as using other distance metrics (e.g. Hausdorff, Chebyshev, etc.), which can improve robustness and global optimisation. In addition, combining other optimisation algorithms such as the DE algorithm and other global search optimisation methods can further improve image registration and avoid local optimal solutions. The DE algorithm can help to overcome local optimal solutions by introducing a global search strategy and find the optimal matches more efficiently over the entire search space with better global optimisation capabilities and robustness, thus improving the challenges in the image registration problem.

Therefore, this paper proposes a feature point matching method based on Hausdorff distance and VPDE. Hausdorff distance measures the "farthest-nearest-distance" between two sets of points to the nearest point of the other set, which makes the method more robust to noise and outliers, especially when there are non-corresponding points in the set of matched points. VPDE is a global optimisation algorithm that searches a wider solution space to avoid local optima. This is especially important for image registration, since there may be multiple local optima in the feature point matching process, and the global optimum is the solution we really want to find.

Assuming 2 sets A and B, the one-way Hausdorff distance from A to B is:

$$h(A, B) = \max_{a \in A} \min_{b \in B} d(a, b) \tag{20}$$

where $d(a, b)$ denotes the Euclidean distance between the points a and b.

The one-way distance from B to A is:

$$h(B, A) = \max_{b \in B} \min_{a \in A} d(a, b) \tag{21}$$

In feature point matching, Hausdorff distance generally refers to the two-way distance and is calculated as shown below:

$$H(A, B) = \max\{h(A, B), h(B, A)\} \tag{22}$$

4. **Experimental results and analyses.**

4.1. **Experimental dataset and experimental environment.**

A good image registration algorithm needs to ensure not only that the number of extracted feature points is sufficiently large, but also that the same feature points can be correctly matched between different images when the image quality changes. Therefore, the image data used

are partly derived from the Mikolajczyk feature matching standard image set and partly from the MATLAB vision toolbox. Detailed information of the experimental data images is shown in Table 1. An example of some of the experimental data images is shown in Figure 4.

Table 1. Experimental data image information

Image Name	sizes	image quality
Bikes	1000 x 700	Image focus blurring
Graf	800 x 640	Perspective change
boat	800 x 640	Zoom + Rotate
Leuven	921 x 614	Light Brightness Change
Building	640 × 480	Perspective change + area overlap

Figure 4. Examples of images of selected experimental data

The experimental platform is MATLABR2020b, the experimental environment is DELI G155511, IntelCorei7-11800H2.3GHz, 8 cores and 16 threads, GPU is NVIDIAGeForceRTX 3060 Laptop6G (GDDR6Micron), 16GB RAM, and the operating system is 64-bit. To verify the performance of the proposed method in this paper, comparative experiments are conducted using SIFT [26], ORB [27], SURF [28], and SURF+VPDE, respectively. The parameter settings of the DE algorithm are shown in Table 2. The main parameters of the VPDE algorithm are $F_{min} = 0$, $F_{max} = 2$, $CR = 0.1$, $G_{max} = 1000$.

Table 2. Experimental parameters

parametric	numerical value
population size	40
The initial scaling factor F	0.6
CR	0.2
D	20
Maximum number of iterations	20000

4.2. **Number of feature points.** The comparison of the number of matching feature points obtained by the four image registration algorithms is shown in Figure 5. It can be seen that for the number of matching feature points, SURF+VPDE > SURF > ORB > SIFT algorithm in the registration process of 5 test samples. The more feature points, the easier it is to obtain effective matching feature point pairs, so the accuracy of the registration can be effectively improved. Whereas, if the number of feature points is too small, it is not conducive to obtaining the features of the global image, and it is not possible to select more feature point pairs, thus reducing the performance of image configuration. Especially for complex and low contrast graph registration, the number of matching feature points is very critical.

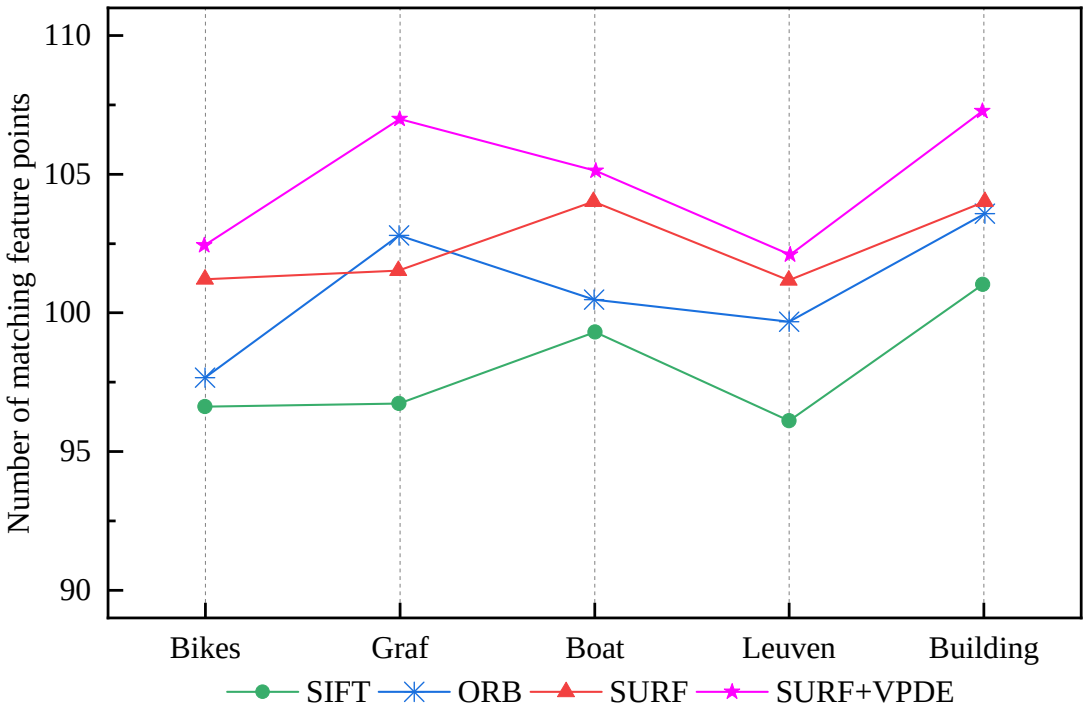

Figure 5. Number of matching feature points

4.3. **Performance impact of VPDE on registration.** In order to verify the performance impact of VPDE on image registration, Hausdorff+DE and Hausdorff+VPDE are used for image registration, respectively. According to the number of correctly matched points, the registration accuracy can be solved and the results are shown in Table 3.

Table 3. Registration accuracy of two algorithms

Image Name	arithmetic	minimum value	average value	maximum value
Bikes	Hausdorff+DE	0.9346	0.9473	0.9664
	Hausdorff+VPDE	0.9875	0.9886	0.9899
Graf	Hausdorff+DE	0.9296	0.9325	0.9535
	Hausdorff+VPDE	0.9818	0.9908	0.9967
boat	Hausdorff+DE	0.9026	0.9153	0.9344
	Hausdorff+VPDE	0.9555	0.9636	0.9681
Leuven	Hausdorff+DE	0.9096	0.9125	0.9335
	Hausdorff+VPDE	0.9618	0.9708	0.9767
Building	Hausdorff+DE	0.8946	0.9073	0.9264
	Hausdorff+VPDE	0.9475	0.9556	0.9631

It can be seen that the accuracy obtained by the VPDE algorithm is higher in terms of registration accuracy. For example, for image bikes, the accuracy of Hausdorff+DE algorithm has a minimum value of 0.9346, a mean value of 0.9473, and a maximum value of 0.9664. whereas the accuracy of Hausdorff+VPDE algorithm has a minimum value of 0.9875, a mean value of 0.9886, and a maximum value of 0.9899. across all images, the Hausdorff+VPDE algorithm has an average accuracy of 0.9662, while the Hausdorff+DE algorithm has an average accuracy of 0.9161. Thus, Hausdorff+VPD improves the accuracy by about 5.5% compared to Hausdorff+DE. This may be due to the fact that after adaptive parameter updating and optimisation of the simulated annealing

algorithm, the DE algorithm's ability to find the optimal value has been improved, and it is able to obtain a higher registration accuracy.

The registration stability tests for Hausdorff+DE and Hausdorff+VPDE will be continued below. After the registration of the five test samples of the experimental data sample set, the RMSE mean value of accuracy is solved and the results are shown in Figure 6.

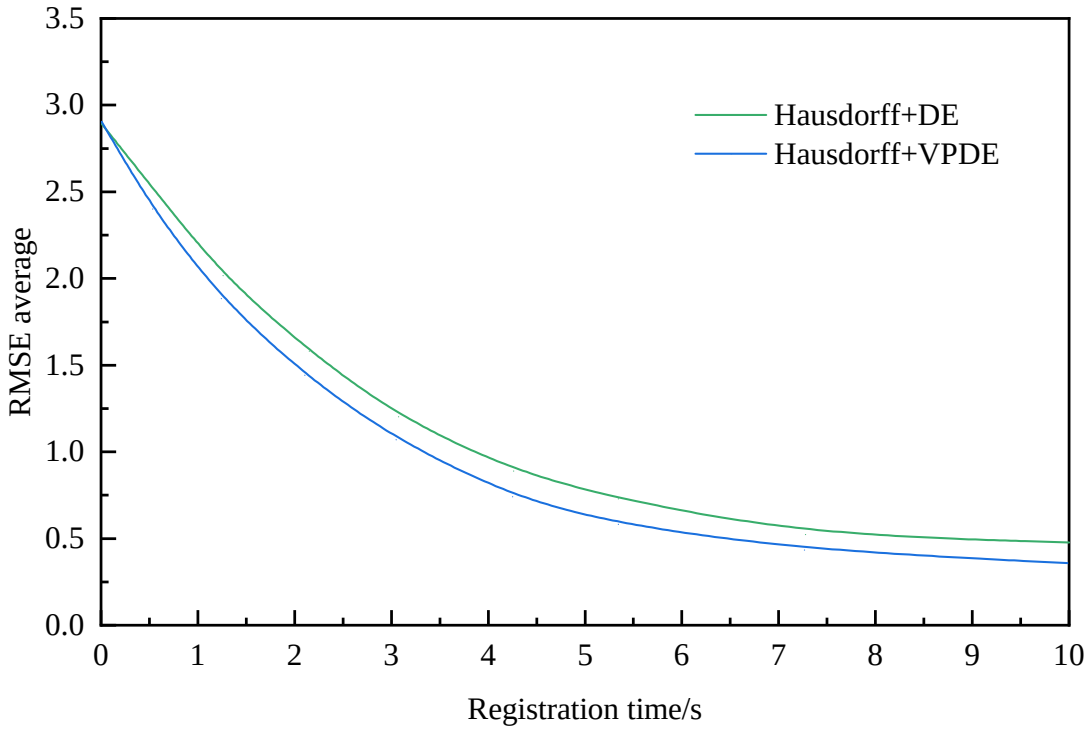

Figure 6. Comparison of RMSE between DE and VPDE algorithms

It can be seen that the VPDE algorithm reduces its registration RMSE value significantly after the variable parameter optimisation with adaptive difference factor. This indicates that after optimisation, the registration stability of the VPDE algorithm is higher. The RMSE value of the VPDE algorithm is finally stabilised at around 0.5. Therefore, after the optimisation of the adaptive parameter update and simulated annealing algorithm, the registration performance of the image is significantly improved and the applicability of the VPDE algorithm in image registration is enhanced significantly.

4.4. **Robustness analysis of different algorithms.** After testing and comparing the matching feature points of the four algorithms, the robustness of the four registration algorithms will be tested and compared in the following, and the results are shown in Table 4.

Table 4. RMSE of four algorithms

arithmetic	Bikes	Graf	boat	Leuven	Building
SIFT	1.2571	1.2784	1.2469	1.2360	1.2348
ORB	0.8628	0.8841	0.8526	0.8417	0.8405
SURF	0.7622	0.7835	0.7520	0.7411	0.7399
SURF+VPDE	0.5067	0.5280	0.4965	0.4856	0.4844

It can be seen that SIFT has the highest RMSE value and worst performance. ORB and SURF have lower RMSE value and better performance. On all the image samples,

SURF+VPDE has the smallest RMSE value and the best performance. The RMSE value of SIFT varies the most among different image samples and the performance is the most unstable. The RMSE value of SURF+VPDE varies less among different image samples and the performance is more stable. Overall, SURF+VPDE is the best and most stable algorithm, ORB and SURF are second only to SURF+VPDE, and SIFT is significantly the weakest in terms of overall performance. The average RMSE of SURF+VPDE algorithm in this experiment is 0.5082, which is significantly lower than the other algorithms.

5. **Conclusion.** In this work, an image registration method based on feature operator and VPDE is proposed. Aiming at the problems of poor robustness and low accuracy of the traditional SURF algorithm, an improved feature operator is proposed. The SURF algorithm uses the 25-dimensional DAISY operator instead of the 64-dimensional SURF operator after obtaining the main direction of the features in the feature description stage, thus reducing the computational complexity. Aiming at the problems of poor robustness and low global optimisation ability of the nearest neighbour KNN matching method based on Euclidean distance, a feature point matching method based on Hausdorff distance and the VPDE algorithm is proposed. The VPDE algorithm uses an adaptive strategy to update the differential scaling factor, and randomly updates the crossover probability using a normal distribution. The experimental results show that the registration performance of Hausdorff+VPDE based images is significantly improved and the applicability of VPDE algorithm in image registration is enhanced significantly. Compared with SIFT, ORB and SURF, SURF+VPDE has the lowest average RMSE of 0.5082, which shows better robustness.

REFERENCES

[1] L. G. Brown, "A survey of image registration techniques," *ACM Computing Surveys (CSUR)*, vol. 24, no. 4, pp. 325-376, 1992.

[2] M. V. Wyawahare, P. M. Patil, and H. K. Abhyankar, "Image registration techniques: an overview," *International Journal of Signal Processing, Image Processing and Pattern Recognition*, vol. 2, no. 3, pp. 11-28, 2009.

[3] B. Zitova, and J. Flusser, "Image registration methods: a survey," *Image and Vision Computing*, vol. 21, no. 11, pp. 977-1000, 2003.

[4] D. L. Hill, P. G. Batchelor, M. Holden, and D. J. Hawkes, "Medical image registration," *Physics in Medicine & Biology*, vol. 46, no. 3, 99, 2001.

[5] M. Deshmukh, and U. Bhosle, "A survey of image registration," *International Journal of Image Processing*, vol. 5, no. 3, 245, 2011.

[6] R. P. Woods, S. T. Grafton, C. J. Holmes, S. R. Cherry, and J. C. Mazziotta, "Automated image registration: I. General methods and intrasubject, intramodality validation," *Journal of Computer Assisted Tomography*, vol. 22, no. 1, pp. 139-152, 1998.

[7] T. Makela, P. Clarysse, O. Sipila, N. Pauna, Q. C. Pham, T. Katila, and I. E. Magnin, "A review of cardiac image registration methods," *IEEE Transactions on Medical Imaging*, vol. 21, no. 9, pp. 1011-1021, 2002.

[8] X. Jiang, J. Ma, G. Xiao, Z. Shao, and X. Guo, "A review of multimodal image matching: Methods and applications," *Information Fusion*, vol. 73, pp. 22-71, 2021.

[9] T.-Y. Wu, H. Li, S. Kumari, and C.-M. Chen, "A Spectral Convolutional Neural Network Model Based on Adaptive Fick's Law for Hyperspectral Image Classification," *Computers, Materials & Continua*, vol. 79, no. 1, pp. 19-46, 2024.

[10] T.-Y. Wu, A. Shao, and J.-S. Pan, "CTOA: Toward a Chaotic-Based Tumbleweed Optimization Algorithm," *Mathematics*, vol. 11, no. 10, 2339, 2023.

[11] L. Yu, D. Zhang, and E.-J. Holden, "A fast and fully automatic registration approach based on point features for multi-source remote-sensing images," *Computers & Geosciences*, vol. 34, no. 7, pp. 838-848, 2008.

[12] G. Hong, and Y. Zhang, "Wavelet-based image registration technique for high-resolution remote sensing images," *Computers & Geosciences*, vol. 34, no. 12, pp. 1708-1720, 2008.

[13] X. Liu, Z. Tian, Q. Lu, L. Yang, and C. Chai, "A new affine invariant descriptor framework in shearlets domain for SAR image multiscale registration," *AEU-International Journal of Electronics and Communications*, vol. 67, no. 9, pp. 743-753, 2013.

[14] A. Singleton, Z. Li, T. Hoey, and J.-P. Muller, "Evaluating sub-pixel offset techniques as an alternative to D-InSAR for monitoring episodic landslide movements in vegetated terrain," *Remote Sensing of Environment*, vol. 147, pp. 133-144, 2014.

[15] S. Wu, W. Zeng, and H. Chen, "A sub-pixel image registration algorithm based on SURF and M-estimator sample consensus," *Pattern Recognition Letters*, vol. 140, pp. 261-266, 2020.

[16] Q. Shi, G. Ma, F. Zhang, W. Chen, Q. Qin, and H. Duo, "Robust image registration using structure features," *IEEE Geoscience and Remote Sensing Letters*, vol. 11, no. 12, pp. 2045-2049, 2014.

[17] F. Ghorbani, H. Ebadi, A. Sedaghat, and N. Pfeifer, "A novel 3-D local DAISY-style descriptor to reduce the effect of point displacement error in point cloud registration," *IEEE Journal of Selected Topics in Applied Earth Observations and Remote Sensing*, vol. 15, pp. 2254-2273, 2022.

[18] Y. Shi, G. Zhao, C. Hu, M. Wang, M. Shi, and H. Ma, "Comparative Study of the Representative Algorithms for Fitting Spherical Target Based on Point Cloud," *IEEE Transactions on Geoscience and Remote Sensing*, vol. 60, pp. 1-16, 2022.

[19] R. Raguram, O. Chum, M. Pollefeys, J. Matas, and J.-M. Frahm, "USAC: A universal framework for random sample consensus," *IEEE Transactions on Pattern Analysis and Machine Intelligence*, vol. 35, no. 8, pp. 2022-2038, 2012.

[20] W. Li, Z. Liang, P. Ma, R. Wang, X. Cui, and P. Chen, "Hausdorff gan: Improving gan generation quality with hausdorff metric," *IEEE Transactions on Cybernetics*, vol. 52, no. 10, pp. 10407-10419, 2021.

[21] M. Pant, H. Zaheer, L. Garcia-Hernandez, and A. Abraham, "Differential Evolution: A review of more than two decades of research," *Engineering Applications of Artificial Intelligence*, vol. 90, 103479, 2020.

[22] W. Deng, S. Shang, X. Cai, H. Zhao, Y. Song, and J. Xu, "An improved differential evolution algorithm and its application in optimization problem," *Soft Computing*, vol. 25, pp. 5277-5298, 2021.

[23] S. Chakraborty, A. K. Saha, A. E. Ezugwu, J. O. Agushaka, R. A. Zitar, and L. Abualigah, "Differential evolution and its applications in image processing problems: A comprehensive review," *Archives of Computational Methods in Engineering*, vol. 30, no. 2, pp. 985-1040, 2023.

[24] W. Deng, J. Xu, Y. Song, and H. Zhao, "Differential evolution algorithm with wavelet basis function and optimal mutation strategy for complex optimization problem," *Applied Soft Computing*, vol. 100, 106724, 2021.

[25] S. Gupta, K. Thakur, and M. Kumar, "2D-human face recognition using SIFT and SURF descriptors of face's feature regions," *The Visual Computer*, vol. 37, pp. 447-456, 2021.

[26] M. Bansal, M. Kumar, and M. Kumar, "2D object recognition: a comparative analysis of SIFT, SURF and ORB feature descriptors," *Multimedia Tools and Applications*, vol. 80, pp. 18839-18857, 2021.

[27] Z. Zhang, L. Wang, W. Zheng, L. Yin, R. Hu, and B. Yang, "Endoscope image mosaic based on pyramid ORB," *Biomedical Signal Processing and Control*, vol. 71, pp. 103261, 2022.

[28] A. Rani, A. Jain, and M. Kumar, "Identification of copy-move and splicing based forgeries using advanced SURF and revised template matching," *Multimedia Tools and Applications*, vol. 80, pp. 23877-23898, 2021.